Genetic and Pharmacological Modulation of Akt1 for Improving Ovarian Graft Revascularization in a Mouse Model 1

Authors: Cohen, Yoni, Dafni, Hagit, Avni, Reut, Fellus, Liat, Bochner, Filip, et al.

Genetic and Pharmacological Modulation of Akt1 for Improving Ovarian Graft Revascularization in a Mouse Model[1]

Yoni Cohen,[3,4] Hagit Dafni,[5] Reut Avni,[3] Liat Fellus,[3] Filip Bochner,[3] Ron Rotkopf,[6] Tal Raz,[7] Laura E. Benjamin,[8] Kenneth Walsh,[9] and Michal Neeman[2,3]

[3]Department of Biological Regulation, Weizmann Institute of Science, Rehovot, Israel
[4]Racine IVF unit, Lis Maternity Hospital, Tel Aviv Sourasky Medical Center, Tel Aviv, Israel
[5]Department of Veterinary Resources, Weizmann Institute of Science, Rehovot, Israel
[6]Department of Biological Services, Weizmann Institute of Science, Rehovot, Israel
[7]Koret School of Veterinary Medicine, Hebrew University of Jerusalem, Rehovot, Israel
[8]Department of Pathology, Beth Israel Deaconess Medical Center and Harvard Medical School, Boston, Massachusetts
[9]Boston University School of Medicine, Department of Medicine, Boston, Massachusetts

ABSTRACT

Ovarian tissue cryopreservation and transplantation is one of a few available treatments for fertility preservation in women diagnosed with cancer. Rapid revascularization is essential for reducing hypoxic damage after grafting and protecting the primordial follicles reserve. Using a mouse model of heterotopic ovarian graft transplantation, we have delineated the role of endothelial Akt1 expression using longitudinal magnetic resonance imaging follow-up to quantify angiogenic response. Endothelial Akt1 activation in ovarian grafts promoted angiogenesis to support the graft during posttransplantation hypoxic period. Similarly, simvastatin therapy activated Akt1 at the transplantation site and improved the revascularization and vascular support of ovarian grafts. These results serve as an important first step toward pharmacological intervention to improve revascularization of ovarian grafts and restoration of fertility in cancer survivors. The pro-angiogenic effects reported here may extend beyond improving ovarian graft reception in fertility preservation and could potentially be used for different organ or tissue transplantation.

Akt1, angiogenesis, fertility, ovarian grafts, preservation, simvastatin

INTRODUCTION

Successful avascular grafting of tissue without surgical connection of blood vessels depends on rapid growth of blood vessels and reestablishment of perfusion. This technique is being used for skin, parathyroid, pancreatic islets, and recently for ovarian grafts. Ovarian tissue cryopreservation and transplantation is one of a few available treatments for fertility preservation in women diagnosed with cancer. Chemotherapy and radiation often have a detrimental effect on the nonrenewable ovarian reserve, leading in many patients to early menopause and increased risk for infertility. Retrieval of ovarian cortex fragments followed by their cryopreservation provides a rapid approach for preservation of fertility. After thawing, cortical ovarian fragments that contain the reserve of primordial follicles are transplanted either orthotopically in the pelvis near the remaining ovaries or heterotopically at the forearm or on the abdominal wall [1]. Unfortunately, this avascular tissue transplantation procedure, without surgical connection of blood vessels, results in a low success rate, mainly due to posttransplantation ischemic injury. Angiogenesis starts on the third day after transplantation, whereas complete blood perfusion is achieved only on Day 6 [2]. Critical loss (up to 70%) of primordial follicles in the first few days after transplantation was reported [3]. Therefore, reducing graft hypoxia and subsequent damage to the ovarian graft is the main goal of research in this field.

The protein kinase Akt1 is the predominant isoform of Akt in endothelial cells. It acts as a principal mediator of angiogenic response, vascular permeability, and vascular maturation [4]. We recently reported that Akt1-deficient ovarian grafts show reduced vascularization and reduced follicular survival [5]. Activation of Akt induces angiogenesis by its anti-apoptotic effects that promote endothelial cell survival, activation of endothelial nitric oxide synthase (eNOS), and regulation of endothelial cell migration and tube formation [6]. Sustained endothelial expression of myristoylated Akt1 (myrAkt1) in normal tissues leads to the development of profound vascular changes, including increased vascular density, blood vessel diameter, and permeability [7, 8]. Furthermore, pharmacological dose-dependent activation of Akt1 can be attained by 3-hydroxyl-3-methylglutaryl coenzyme A reductase inhibitors, also known as statins [9].

As part of our constant search for an efficient method to induce active angiogenesis at the site of ovarian graft transplantation, we used dynamic contrast-enhanced magnetic resonance imaging (MRI) to track angiogenic biomarkers in ovarian graft following tetracycline-inducible endothelial expression of Akt1. Based on the positive effects of Akt1 overexpression, we investigated whether pharmacological induction of Akt1 by statins can improve blood vessel formation, accelerate reperfusion, and ultimately improve ovarian graft reception.
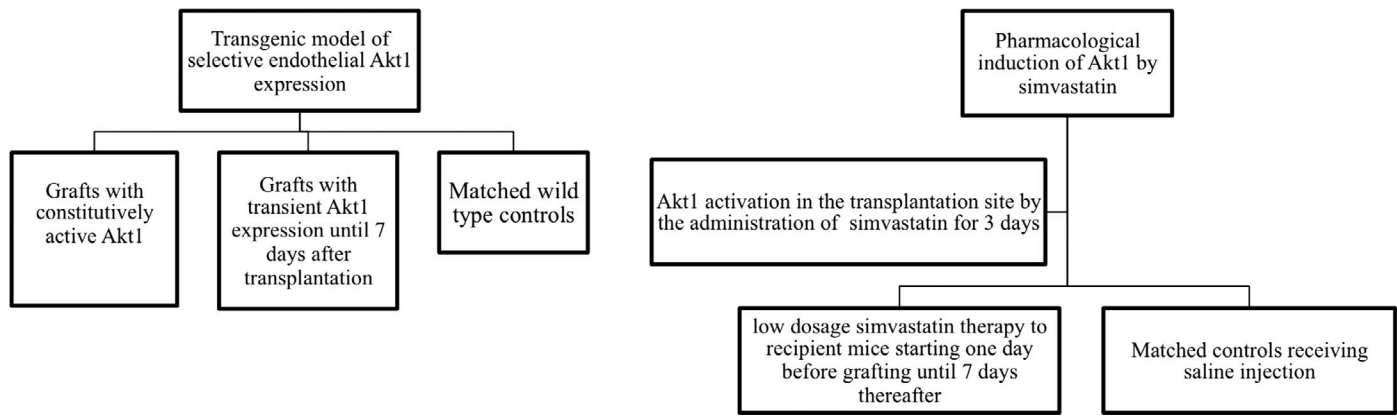
FIG. 1. Flow chart of the study showing the experimental design.

MATERIALS AND METHODS

Animal experiments were approved by the Weizmann Institutional Animal Care and Use Committee. The experimental design is shown in Figure 1.

Ovarian Graft Retrieval

Ovaries were collected from donor mice at the beginning of their sexual maturity, at 5–6 wk of age. The following three mouse strains were used in this study: 1) Mice with transgenic tetracycline-repressible endothelial-specific Akt1 activation under the VE-cadherin promoter (VE-cadherin-tTA;TET-myrAkt1) were received from Professor Laura E. Benjamin (Department of Pathology, Beth Israel Deaconess Medical Center, and Harvard Medical School) [8]. Ovarian grafts were retrieved 4 days after induction of expression of myrAkt1 in the donor animals by removal of tetracycline from the drinking water. Ovarian grafts from TET-myrAkt1-negative mice were used as matching controls; 2) Mice that express tdTomato red fluorescent protein in endothelial cells under the VE-cadherin promoter, that is, B6.Cg-Gt (ROSA)26Sor < tm14 (CAG-tdTomato)Hze > /J (Jackson Laboratory); and 3) C57BL/6 black wild-type mice (Harlan Laboratories).

Mice were euthanized using CO_2 inhalation, and ovaries were collected and cleaned of fat and other tissues in a PBS solution maintained at 37°C. This model focuses on angiogenesis and vascular remodeling during the critical ischemic interval posttransplantation, and thus, we used a fresh ovarian graft that was transplanted within 15 min from retrieval to minimize preimplantation ischemic damage to the tissue.

Ovarian Graft Transplantation

Ovarian grafts were transplanted in 6- to 9-wk-old CD-1 nude female mice (Harlan Laboratories). At 2–3 wk prior to ovarian tissue transplantation, recipient mice underwent ovariectomy under anesthesia with 100 mg/kg ketamine and 20 mg/kg xylazine, injected intraperitoneally. Two different transplantation sites were used in this study: 1) Intramuscular ovarian graft transplantation was applied for in vivo dynamic contrast-enhanced MRI. A 5 mm incision was made in the biceps femoris muscle of the thigh, 5 days prior to transplantation, to form granulation tissue at the site of implantation. It was previously reported that transplantation into granulation tissue improves graft revascularization [10]. On the day of ovarian graft transplantation, the surgical incision in the biceps femoris muscle was cleaned of blood clots and debris and rinsed with PBS. Then the ovary was transplanted intramuscularly at the site of the granulation tissue created by the incision 5 days earlier. The edges of the muscle were closed over the graft with 7/0 Prolene sutures (Ethicon), taking care not to traverse and damage the ovarian tissue. Skin incision was closed with 5/0 Mersilk sutures (Ethicon) and covered with Super Glue Gel (ethyl cyanoacrylate; Loctite) to seal the wound. 2) Intraperitoneal transplantation was applied for fluorescent imaging. The peritoneal surface was exposed through a midline laparotomy incision. Ovarian grafts were anchored to the parietal peritoneum with 7/0 Prolene sutures. The peritoneal cavity was closed with continuous sutures of 5/0 Mersilk. The skin was closed with interrupted 5/0 Mersilk sutures and sealed with Super Glue Gel.

Drug Interventions

Superovulation was induced 30 days after transplantation. Mice were subcutaneously injected with 5 units of equine chorionic gonadotropin (eCG) (National Hormone & Peptide Program, Harbor-UCLA Medical Center) dissolved in 100 ml of PBS. Five units of human chorionic gonadotropin (hCG) (Sigma Aldrich) was intraperitoneally injected to the animals 48 h after the eCG [11]. Ovarian grafts were monitored using MRI.

Activation of Akt by simvastatin was tested in 0.1 and 1mg/kg doses by ex vivo immunoblotting (see below). To activate the simvastatin prodrug (Sigma), 4 mg of simvastatin was dissolved in 100 µl of ethanol. Then, 150 µl of 0.1 N NaOH was added to the solution that was subsequently incubated at 50°C for 2 h. The pH was brought to 7.0 by HCl, and the final concentration of the stock solution was adjusted to 4 mg/ml. The stock solution was kept at 4°C [12]. Recipient mice received daily intraperitoneal (IP) injections of low-dose simvastatin (0.1 mg/kg/day) or saline, starting 1 day before grafting until 7 days thereafter, when complete reperfusion is expected [2]. Ovarian grafts were monitored using MRI.

In Vivo Dynamic Contrast-Enhanced MRI of Ovarian Grafts

MRI experiments were performed at 9.4 T on a horizontal Biospec spectrometer (Bruker), using a linear coil for excitation and a 2 cm surface coil for detection (Bruker). Animals were anesthetized with isoflurane (3% for induction, 1%–2% for maintenance); (Abbott Laboratories Ltd.) in oxygen (1 L/min) delivered through a muzzle mask and kept under respiratory monitoring. Body temperature was maintained using a heated bed.

Recipient mice were serially scanned at predefined time intervals: Day 2 to obtain a baseline during the ischemic period of the graft; Day 7 at the end of the ischemic period when graft reperfusion is expected; Day 30 before superovulation (pre-eCG/hCG); and Day 33 after superovulation was completed (post-eCG/hCG). During MRI experiments, the macromolecular contrast agent biotin-bovine serum albumin-gadolinium diethylenetriamine-pentaacetic acid (biotin-BSA-GdDTPA) (10 mg/mouse in 0.2 ml of PBS; SyMO-Chem BV) was injected through a tail vein silicone catheter. Three-dimensional (3D)-gradient echo images of the graft were acquired before and sequentially for 40 min after intravenous administration of the contrast agent. Precontrast, T1-weighted, 3D-gradient echo images were acquired with variable flip angle (repetition time: 10 msec; echo time: 2.8 msec; flip angles: 5°, 15°, 30°, 50°, 70°; two averages; matrix: $256 \times 256 \times 64$; field of view: $35 \times 35 \times 35$ mm). Postcontrast images were carried with a single flip angle (15°).

Analysis of Dynamic MRI Data

Pixel by pixel analysis was performed using Matlab software (Math Works Inc.) to generate R1 maps and consequently concentration maps of biotin-BSA-GdDTPA in the grafts and surrounding tissues for selected slices. Vascular properties were derived from the dynamics of contrast agent accumulation [13].

Blood volume fraction (fBV). The ratio between the extrapolated concentration of contrast agent in the tissue at the time of administration and the initial concentration in the blood.

Permeability surface area product (PS, 1/min). We measured the initial rate of contrast accumulation normalized to initial blood concentration. PS reflects leakage of the macromolecular contrast agent out of the vascular compartment and its accumulation in the interstitial space.

Mean fBV and PS values were calculated for each graft, from parameter maps, by manually drawing regions of interest encompassing the graft in all relevant slices of the 3D data set.

Mapping the Origin of Ovarian Graft Blood Vessels with Fluorescence Microscopy

At 1 wk after transplantation, VE-cadherin-tdTomato ovarian grafts that were grafted on the parietal peritoneum were imaged using a Zoom Stereo Microscope SZX-RFL-2 (Olympus), equipped with a fluorescence illuminator and a Pixelfly camera (PCO), and analyzed using ImageJ software (http://rsbweb.nih.gov/ij/). To map both host (peritoneal) and graft endothelial cells in functional blood vessels, dextran-fluorescein isothiocyanate (FITC) (500 kDa; Sigma Aldrich) was injected (3 mg/mouse in 0.1 ml PBS) via a tail-vein catheter. The host peritoneal blood vessels were depicted after exposure of the peritoneal surface by the signal of FITC in their lumen (green). Graft-derived vascular endothelial cells were identified by the red signal of the tdTomato protein.

To confirm that the tdTomato signal originated from the graft's endothelial cells, the flow inside the blood vessels was imaged noninvasively in vivo with Laser Speckles Imaging [14]. The endothelial cells were imaged in vivo using the tdTomato expression under the VE-cadherin promoter in transgenic mice. In vivo imaging of the ovary was performed in the ovarian imaging window, a tissue preparation enabling intravital longitudinal imaging of the mouse ovary [15].

To image the endothelial cells together with contrast material inside the lumen of blood vessels, 2 mg of 500 dextran-FITC (Sigma-Aldrich) was injected intravenously into a tail vein through a catheter. The ovarian vasculature was imaged shortly after the injection ex vivo with two-photon microscope (LSM 880 Zeiss Laser Scanning Microscope; Carl Zeiss). The imaging revealed tdTomato fluorescence in endothelial cells and FITC signal inside the lumen.

Histological Assessment of Microvascular Density, Permeability, and Follicle Count

Ovarian graft and surrounding muscle were retrieved for histology at the end of the last serial MRI session, approximately 40 min postinjection of biotin-BSA-GdDTPA. Prior to tissue retrieval, additional contrast material, bovine serum albumin (BSA), labeled with a rhodamine derivative (ROX; Invitrogen) [16], was injected through the tail vein catheter (2.5 mg/mouse in 0.2 ml PBS). Animals were sacrificed 2 min after the administration of BSA-ROX such that it remained inside the lumen of blood vessels with minimal leakage.

To preserve the biotin and fluorescent tags, retrieved tissue was placed in Carnoy fixative solution (6:3:1 ethanol:chloroform:acetic acid) for 24 h at 4°C and then transferred to 70% ethanol. The fixed samples were embedded in paraffin blocks and sectioned serially at 4 μm thickness. Morphometric data was obtained by multilevel sampling of the graft at 120 μm intervals.

Density of functional blood vessels was assessed directly from the fluorescent signal of the intravascular BSA-ROX. Vascular density was derived from five representative histological midsections and normalized by dividing the density of pixels with fluorescent signal above a predefined threshold in the graft to that in the adjacent muscle. Permeability was assessed from the distribution of the extravasated biotin-BSA-GdDTPA, visualized by staining the histological sections with avidin-CY2 conjugate (Jackson Laboratory). Images were obtained with a Zeiss Axio observer microscope equipped with a fluorescence illuminator and an Olympus DP72 camera and analyzed using ImageJ software.

Immunohistochemical staining was used for assessment of maturation of blood vessels according to the degree of coverage with α-smooth muscle actin (αSMA)-expressing perivascular pericytes or vascular smooth muscle cells. After deparaffinization, slides were incubated overnight at 4°C with αSMA antibodies (1:500; Novus Biologicals) and were detected using a second antibody conjugated with alkaline phosphatase (Jackson Laboratory) and its substrate, Fast Red (Sigma). Slides were counterstained with Mayer hematoxylin solution. Slides were examined with a Nikon Eclipse E800 microscope.

Follicle count. Follicular reserve was assessed by serial multilevel histological sections, with 120 μm gap between levels and stained with hematoxylin and eosin (H&E). Both healthy and atretic follicles were counted and classified according to the type. The follicle density per cubic millimeter was calculated using ovarian graft volume measured by MRI. Follicle density was also corrected for the nonvascular ovarian tissue by measuring the fluorescence signal of intravascular BSA-ROX.

Immunoblot Analysis of Akt1 Activation by Simvastatin

C57BL/6 female mice received IP injection of 0.1 or 1 mg/kg simvastatin or saline once daily for 3 days (n = 5 for each treatment group). Protein was extracted on the fourth day from the thigh muscle using meticulous tissue dissociation and phosphatase inhibitors in order to preserve the active phosphorylated form of Akt. Cell lysates were resolved by SDS-PAGE (10%) followed by Western immunoblot analysis, using rabbit polyclonal anti-phosphorylated Ser473 residue of Akt antibody (1:1000; Cell Signaling Technologies). To verify the amount of loaded proteins and inactivated fraction, blots were reprobed with rabbit polyclonal anti-Akt1 antibody (1:1000; Santa Cruz). To explore the effect on eNOS, blots were probed with rabbit monoclonal anti-eNOS (Ser1177) antibody (1:1000; Cell Signaling Technologies).

Statistical Analysis

PS and fBV data were analyzed using repeated-measure ANOVA. The effect of genotype or simvastatin administration was analyzed with simvastatin treatment as a between-subject factor and with the effect of individual mice nested within the treatment factor. Where comparisons were made within a single day, a nested ANOVA model was used with the effect of individual mice nested within the treatment factor. Follicle counts were compared using an independent-samples t-test. Western blot data was analyzed using a one-way ANOVA followed by a Tukey post hoc test. Differences were considered significant at $P < 0.05$. Results are presented as mean ± SEM. All statistical analyses were performed using Statistica, version 12 (Statsoft, Inc.).

RESULTS

Depicting the Dynamics of Ovarian Graft Reperfusion Using In Vivo Imaging

Graft-induced vascular remodeling was followed longitudinally using a macromolecular blood-pool contrast agent (biotin-BSA-GdDTPA), which extravasates specifically from newly formed hyperpermeable blood vessels. Ovarian grafts showed severe ischemia 2 days after grafting followed by recovery of perfusion 5 days later (Fig. 2, A and B). MRI-derived blood volume (fBV) gradually improved from baseline measurement on Day 2 until 30 days posttransplantation, with an additional increase after hormonal induction of ovulation using eCG/hCG (Fig. 2C). As the graft's newly formed blood vessels matured, mean vessel permeability (PS) declined from Day 2 until Day 30. It modestly increased after eCG/hCG administration (Fig. 2D).

To learn more about the origin of the graft blood vessels, ovarian grafts that express tdTomato red fluorescent protein in their endothelial cells (VE-cadherin-tdTomato) (Supplemental Fig. S1; Supplemental Data are available online at www.biolreprod.org) were grafted intraperitoneally. Most of the graft's vasculature, especially in the center of the graft, originated from the graft. A fine network of recipient-peritoneal blood vessels invaded the graft's periphery (up to one-third of the cross-sectional length of the graft) (Fig. 2, E–G). Most importantly, in all grafts, we observed graft blood vessels that sprouted radially, from the grafts toward the recipient peritoneal vasculature to create functional anastomosis (Fig. 2, H and I).

Selective Activation of Endothelial Akt1 Expression Induces Enhanced Posttransplantation Angiogenic Response in Ovarian Grafts

To explore the role of endothelial Akt1 in graft reception, ovarian grafts with tetracycline-regulated expression of activated Akt1 selectively in endothelial cells (VE-cadherin-myrAkt1) were transplanted into the thigh muscle. Mean fBV was significantly higher from 7 up to 30 days after grafting. Mean fBV increased by almost 400%, compared to the baseline
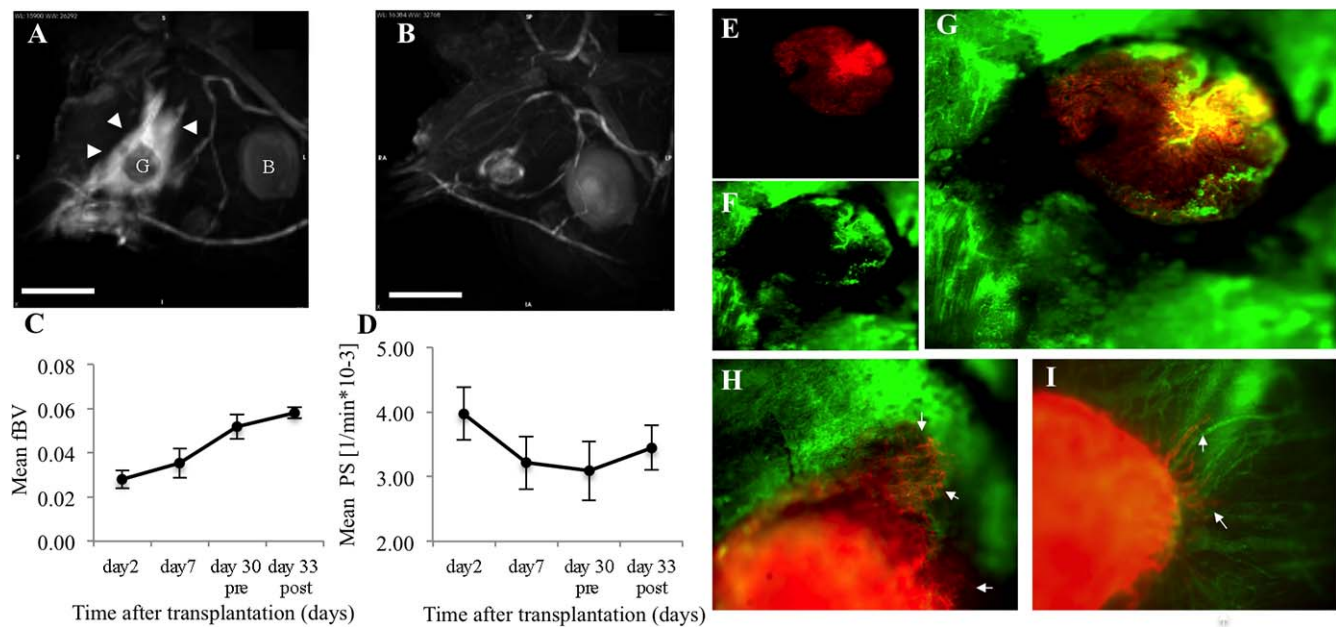
FIG. 2. The dynamics of ovarian graft reperfusion. **A**–**D**) Ovarian graft harvested from C57/B wild-type mice were transplanted in the thigh muscle of recipient mouse. Three-dimensional contrast-enhanced MRI revealed the transition of ovarian graft from the ischemic period 2 days after grafting (**A**), characterized by minimal filling of the graft's vasculature and extravasation of contrast agent from leaky peripheral blood vessel (arrowheads), to reperfusion 7 days thereafter (**B**). Reperfusion is marked by contrast enhancement in the graft vasculature with minimal leakage to the surrounding muscle. Maximal intensity projections presented here were acquired 40 min after intravenous injection of biotin-BSA-GdDTPA. G = ovarian graft; B = urinary bladder. Bar = 5 mm. MRI-derived vascular parameters reflects the changes in blood volume fraction (mean fBV; **C**) and vessel permeability (mean PS; **D**) over time. The graft's new vasculature is characterized by gradual increase in fBV (**C**) and gradual decrease in PS (**D**) over time. Pre-MRI on Day 30 was performed prior to eCG/hCG-induced superovulation. Post-Day 33, 14–17 h after hCG administration. Data presented as mean ± SEM (n = 7). **E**–**I**) Ovarian grafts with red fluorescent endothelial cells (from a VE-cadherin-tdTomato donor) were transplanted on the recipient peritoneum. Stereomicroscope images acquired 7 days after grafting show that ovarian graft vasculature originates predominantly from the graft's endothelial cells, depicted by the tdTomato fluorescence signal (red; **E**). Perfused blood vessels in the graft and surrounding peritoneum are highlighted by intravenous injection of dextran-FITC (green; **F**). Overlay images (**G**–**I**) show that most of the grafts vasculature, mainly in the center of the graft, originated predominantly from the graft's own vasculature (red). Some of the vessels were perfused as evident by the colocalization of FITC and tdTomato signals (yellow). A fine network of peritoneal blood vessels (green) invaded the periphery of the graft. **H**, **I**) Two representative slides showing ovarian graft blood vessel outgrew (red) toward the peritoneal vasculature (green) to create anastomosis (arrows). Original magnification ×40 (**E**–**I**).

level, on Day 2 and remained relatively constant on Days 7, 14, and 30. Mean fBV in the controls increased by 46%–87% on Days 7–30 (Fig. 3, A–D). Mean PS of VE-cadherin-myrAkt1 grafts was gradually reduced over time, albeit at a slower rate compared to controls and was significantly higher 14 days after transplantation (Fig. 3E). The development of this new vasculature in myrAkt1 was accompanied by a significant increase in graft volume compared to controls (Fig. 3F).

The morphological changes that resulted in these very high fBV values were clearly evident in histological sections. Ovarian tissue, including follicles and stroma, was enclosed by numerous, abnormally appearing blood vessels characterized by large diameter blood lakes and tortuous vessels (Fig. 4A). All myrAkt1 grafts contained antral follicles, and 66% of the myrAkt1 grafts that were assessed were at least partially functional, as was evident by the presence of corpora lutea. The transplantation site consisted of two morphologically distinct blood vessels: 1) numerous normal blood vessels in the muscle adjacent to the graft and 2) large aberrant blood vessels in the graft, congested with erythrocytes. Compared to controls, (Fig. 4, E and F), some of the large stromal blood vessels in myrAkt1 grafts were mature and expressed αSMA, while this marker was not found in some of the immature ones (Fig. 4, C and D). Thirty days after grafting of myrAkt1 grafts, although PS values were similar to controls, some of the newly formed abnormal vessels lacked mural cell support. Using fluorescence microscopy, we recorded high signal intensity of BSA-ROX (indicating perfused vasculature) in abnormally enlarged blood

vessels inside myrAkt1 grafts. Furthermore, the area of the grafts that was covered by patent blood vessels was, on average, 72.86% ± 8.50% in myrAkt1 compared to 39.14% ± 6.74% in controls ($P < 0.05$ by t-test; myrAkt1 n = 3 vs. control n = 6; Fig. 4, G–J).

So far, we showed that long-term constitutively active Akt1 improved the vascularity of the graft. Physiologically, pro-angiogenic factors are required during the first week after transplantation. After that period, the graft should be adequately perfused. To assess if transient expression of myrAkt1 can be used to improve ovarian graft reception, expression of myrAkt1 was suppressed 7 days after transplantation (myrAkt1[transient]). As expected, 7 days after transplantation myrAkt1[transient] grafts had significantly higher fBV and also showed a trend toward higher PS values. At this point in time, myrAkt1 was suppressed by addition of tetracycline to the drinking water; consequently, on the following scans, fBV and PS values returned to a level similar to the controls. The myrAkt1[transient] and control grafts responded similarly to eCG/hCG, by increasing their fBV, while PS showed a small decrease and increase in myrAkt1[transient] and controls, respectively (Fig. 5, A–D).

Follicular reserve was estimated by multilevel histological sections. We found no differences in primordial, primary, secondary antral corpora lutea and atretic follicle counts and follicle density per cubic millimeter (Fig. 5, E and F). One month after transplantation (3 wk after myrAkt1 suppression), myrAkt1[transient] ovarian grafts were adequately perfused and
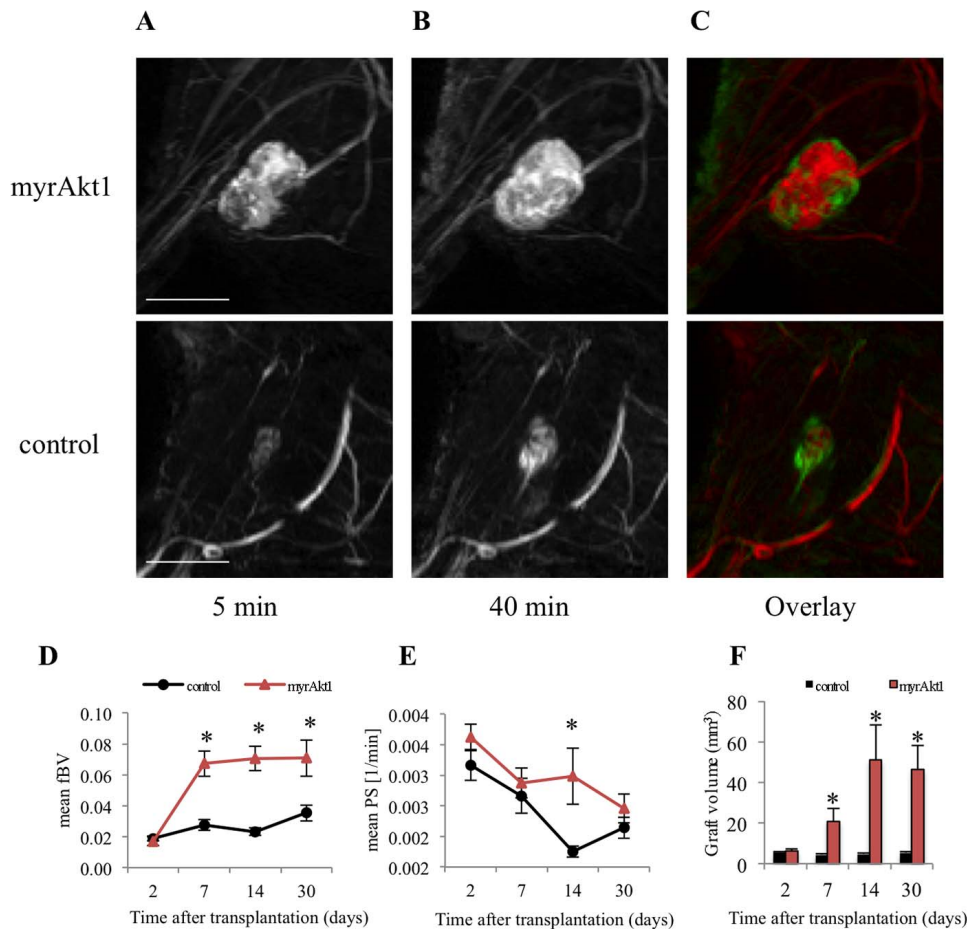
FIG. 3. Changes in fBV, PS, and graft volume over time in myrAkt1 and control grafts. **A–C**) Maximal intensity projections of dynamic contrast-enhanced MRI in myrAkt1 and control grafts 7 days after transplantation. Images show early vascular filling at the first scan, 5 min after the injection of biotin-BSA-GdDTPA (**A**), contrast agent extravasation (permeability), and accumulation 40 min postinjection (**B**), and overlay image of the 5 min (red) and 40 min (green) time points (**C**). Bar = 5 mm. **D**) Mean blood volume fraction (fBV) was significantly higher in myrAkt1 grafts compared to controls from Day 7 onward. **E**) Mean vessel permeability (PS) decreases gradually in both groups. However, PS was significantly higher in myrAkt1 grafts on Day 14. **F**) Mean volume of myrAkt1 ovarian grafts (measured from MRI) was significantly higher from Day 7 onward (n = 9 for myrAkt1; n = 5 for control). *$P < 0.05$ by nested ANOVA (**D**, **E**) and by independent t-test (**F**). Data presented as mean ± SEM.

developed extensive vascularity within the graft's stroma (Supplemental Fig. S2).

Improved Ovarian Graft Angiogenesis by Pharmacological Induction of Akt1

In the next step, we tested whether the administration of a 3-hydroxyl-3-methylglutaryl coenzyme A reductase inhibitor, that is, simvastatin, to the recipient can activate Akt1 at the transplantation site and thus improve ovarian graft reperfusion. First, we tested whether Akt1 can be activated in the muscle by the administration of 0.1 and 1 mg/kg simvastatin for 3 days. This treatment caused a 3-fold increase in Akt phosphorylation on Ser473 ($P < 0.05$). Raised phosphorylated Akt level was correlated with a downstream increase in phosphorylated eNOS (Ser1177). Simvastatin administration caused an approximate 3- and 7-fold increase in phosphorylated eNOS at 0.1 and 1 mg/kg dosage, respectively ($P < 0.05$) (Fig. 6).

Following this successful induction of activated Akt in the transplantation site, we assessed whether low dosage (0.1 mg/kg/day) simvastatin therapy starting 1 day before grafting until 7 days thereafter can improve ovarian graft vascularization. Variations in fBV and PS values of each voxel within the graft were recorded for each animal at 2, 7, and 30 days after

grafting. We found a significant effect of simvastatin treatment on improved blood volume fraction in ovarian transplants. On Day 7, mean fBV was significantly higher in the simvastatin group. Grafts treated with simvastatin improved their mean fBV values by 80% ± 5% compared to baseline levels on Day 2, while mean fBV improved by only 21% ± 3% in the control group ($P < 0.05$ n = 7 in each group). Mean PS was significantly higher on Day 2 in the simvastatin group, which can be explained by augmented angiogenic response and increased permeability of new blood vessels, in contrast to lower mean PS levels on Day 7, which represents accelerated maturation in the simvastatin group (Fig. 7, A and C).

MRI-derived fBV and PS values were also used to dynamically test angiogenic response in ovarian grafts following superovulation with eCG/hCG. In order to support the massive formation of new blood vessels after ovulation induction, the graft needs an adequate scaffold of blood vessels that will be able to perfuse growing follicles and corpora lutea. Mean fBV significantly increased in the simvastatin group compared to prehormonal levels (60% ± 3.20% vs. 28% ± 2.19% increase in simvastatin and control groups, respectively, $P < 0.05$, n = 7 in each group). This increase in fBV was coupled with a decrease in PS after eCG/hCG (Fig. 7, B and D).
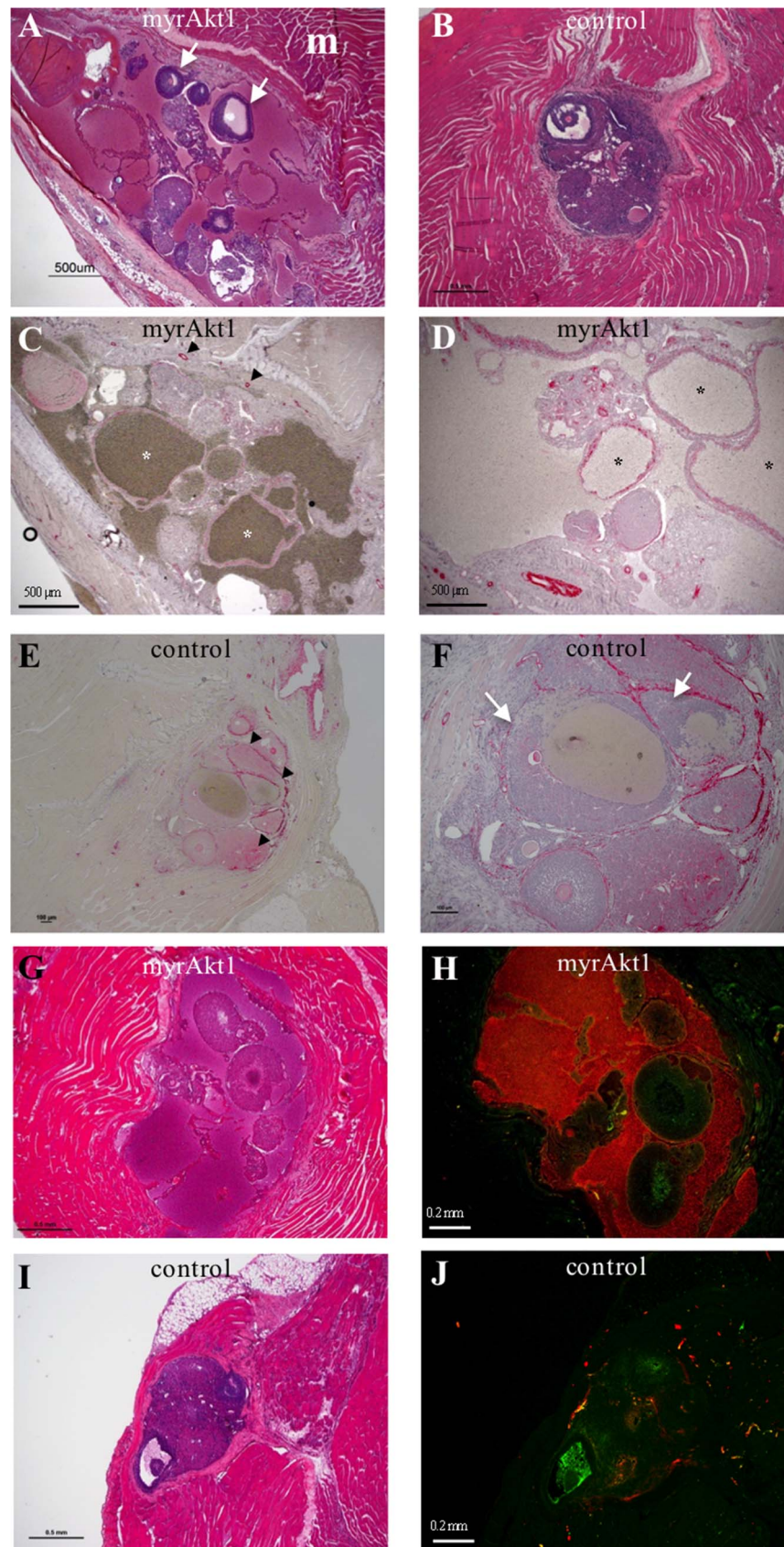
5

FIG. 4. Increased vascularity and abnormal growth of irregular blood vessels in myrAkt1 ovarian grafts. **A**, **B**) H&E staining 30 days after grafting. Ovarian tissue of myrAkt1 graft, including follicles and stroma, was enclosed in numerous, abnormally appearing blood vessels characterized by large diameter and tortuous vessels (**A**). Controls showed normal morphology of ovarian graft (**B**). Arrow = antral follicles, m = muscle. **C–F**) Alpha smooth muscle actin (α-SMA) staining (red). **C**, **D**) Two different areas in myrAkt1 graft showing maturation of large diameter blood vessels in myrAkt1 graft (*) with a thickened wall. Arrowheads = normal blood vessels in the border between the muscle and graft. **E**, **F**) Controls, normal blood vessels distribution in the graft and
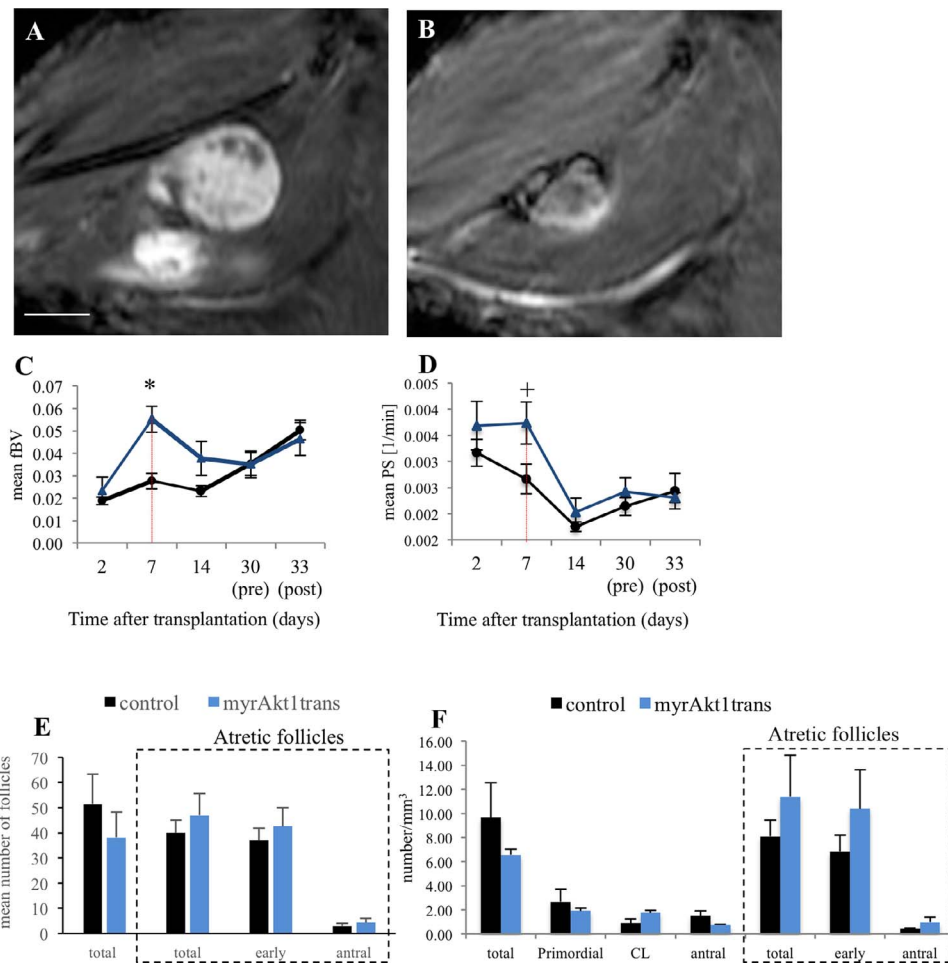
FIG. 5. Angiogenic response to transient induction of myrAkt1 in ovarian grafts. **A**, **B**) Representative contrast-enhanced MRI of myrAkt1 graft taken 40 min after injection of contrast agent. The high signal intensity and accumulation observed in ovarian graft 7 days after grafting (**A**) diminished in volume and extent by Day 14, which is 7 days after the suppression of myrAkt1 (**B**; same graft as in **A**). Bar = 5 mm. Elevated mean blood volume fraction (fBV; **C**) and mean vessel permeability (PS; **D**) in myrAkt1 ovarian grafts 7 days after grafting gradually return to control values after myrAkt1 suppression. Red dashed line indicates time of myrAkt1 suppression. MRI on Day 30 was performed prior to eCG/hCG-induced superovulation and repeated on Day 33, 14–17 h after hCG administration. **E**, **F**) Ovarian graft follicle count and follicle density. No differences were found in follicle counts and density 33 days after grafting; n = 5 (transient induction of myrAkt1, myrAkt1trans), n = 9 (controls). CL = corpora lutea. Early-immature follicles up to the secondary stage. *$P < 0.05$, +$P = 0.06$ (trend) by nested ANOVA (**C**, **D**) and by independent t-test (**E**). Data presented as mean ± SEM.

Next, we wanted to assess vascular density in histological sections retrieved at the end point of the study on Day 33 after eCG/hCG. The ratio of pixels with a BSA-ROX signal above a predefined threshold inside the graft, to those in the surrounding muscle, was calculated in five histological sections representing different areas within the graft. Normalized blood vessel density in the grafts treated with simvastatin was 33 ± 5.6 times higher than the muscle, compared to only 16 ± 0.97 times higher in the controls ($P < 0.05$) (Fig. 8, A–E). This serves as further proof of improved vascular support in ovarian grafts treated with simvastatin. Follicle counts showed an increase in corpora lutea density, while no differences were found in ovarian graft volume. Furthermore, grafts in the simvastatin group had a lower number of atretic follicles (Fig. 8, F and G, and Supplemental Fig. S3).

DISCUSSION

Ovarian grafts show severe posttransplantation ischemia and regain their perfusion at the end of the first week posttransplantation [2, 17, 18]. Decreasing posttransplantation ischemia will protect the primordial follicles reserve and increase the probability for achieving pregnancy. This study delineates the physiological vascular changes in ovarian grafts and enhanced angiogenesis after transgenic endothelial Akt1 activation. Similarly, pharmacological activation of Akt1 by simvastatin improved the revascularization of ovarian grafts.

Akt1 is a principal mediator in the PI3K signaling pathway, controlling angiogenesis by a composite downstream signaling network [19]. Recently, we reported deficient posttransplantation angiogenic response reflected by a gradual decrease in microvascular density after transplantation of Akt1-deficient

surrounding muscle. Arrowheads = normal blood vessels surrounding growing follicles and inside a corpus luteum. Arrows = antral follicles. **G–J**) High blood volume in abnormally enlarged vessels inside myrAkt1 graft. H&E staining (**G**, **I**). Fluorescence microscopy (**H**, **J**): red = BSA-ROX injected 1 min prior to animal sacrifice; green = extravasation of avidin-CY2-biotin-BSA-GdDTPA from permeable blood vessels injected 40 min prior to animal sacrifice and visualized using avidin-CY2. Bars = 500 μm (**A**, **C**, **D**), 0.5 mm (**B**, **G**, **I**), 100 μm (**E**, **F**), and 0.2 mm (**H**, **J**).
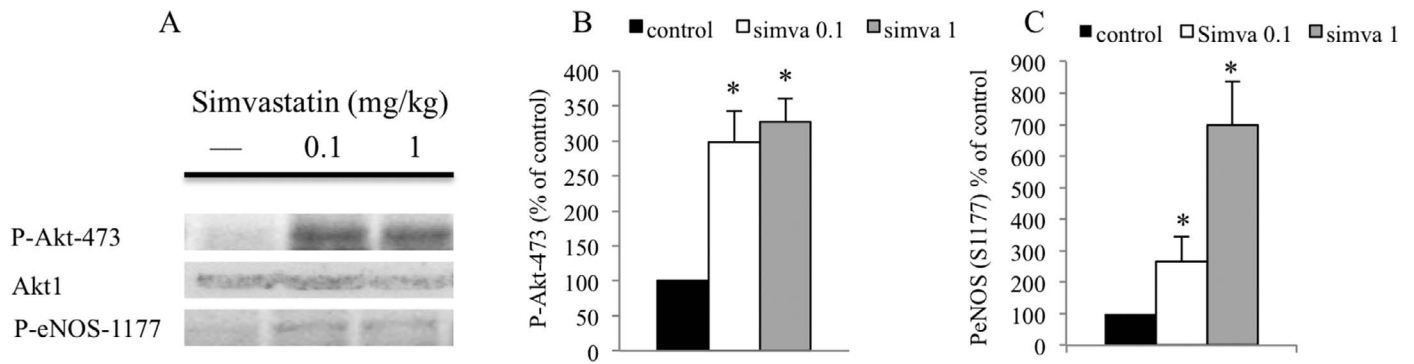
FIG. 6. Induction of activated Akt1 and eNOS in the muscle after 3 days of simvastatin therapy. **A**) Western immunoblot of p-Akt (Ser473), p-eNOS (Ser1177), and total Akt1 in muscle lysate from c57/B mice treated with daily intraperitoneal injections of 0.1 and 1 mg/kg simvastatin or saline for 3 days. **B**) Quantitative Western blot densitometry results showing that simvastatin administration caused a 3-fold increase in p-Akt (Ser473) relative to control. **C**) Simvastatin administration caused approximately 3- and 7-fold increase in phosphorylated eNOS at 0.1 mg/kg and 1 mg/kg respectively (n = 5 animals in each group). *$P < 0.05$ by one-way ANOVA followed by a Tukey post hoc test. Data presented as mean ± SEM.

ovarian grafts [5]. However, in these transgenic grafts, all cells lost Akt1 expression; therefore, other cellular mechanisms beyond graft hypoxia and vascular remodeling could have impaired graft reception. On Day 60, Akt1-deficient grafts exhibited abnormal vascular changes coupled with reduced perfusion that indicate a primary angiogenic defect. In this study, we focused on vascular events by using an endothelial-specific transgenic Akt1 modulation. As reported here, selective endothelial Akt1 activation amplified the angiogenic response and vascular remodeling in ovarian grafts. The area of the graft covered by blood vessels in myrAkt1 grafts was almost double that of the controls. Follicles and ovarian stromal tissue were surrounded by large aneurysmal-like blood vessels, while fBV increased 4-fold, relative to the baseline level on Day 2, and remained high as long as myrAkt1 was induced. This massive increase in blood volume was accompanied by increased permeability (PS). This newly formed vasculature can reduce tissue hypoxia and improve diffusion of other molecules by increasing both vessel surface area and permeability. But perhaps more importantly, accelerating angiogenesis immediately after implantation could reduce posttransplantation hypoxia and follicular loss. However, even chronic Akt1 overexpression led to some degree of blood vessel maturation, as was evident by a gradual decrease in PS over time and a return to a level similar to controls 30 days after transplantation. Mural support of these newly formed aberrant blood vessels was not uniform. In some of the enlarged blood vessels in myrAkt1 grafts, we found a high expression of αSMA in the vessel wall, while other vessels had only partial mural support. These findings can explain both the increased extravasation rate of the contrast agent in myrAkt1 grafts as well as blood vessel maturation over time.

Unlike loss of Akt1, selective endothelial Akt1 expression improved vascular support to ovarian graft compared with the controls. Nevertheless, the massive increase in blood perfusion and tissue edema that was recorded in myrAkt1 grafts might negatively affect ovarian endocrine function and follicular maturation. Physiologically, pro-angiogenic factors are required during the first week after transplantation [2]. After that period, the graft should be adequately perfused. Endothelial activation of myrAkt1 transiently for 7 days resulted in augmented angiogenesis and recovery by 30 days of normal graft morphology.

The distinctive vascular phenotype that develops in myrAkt1 grafts is in accordance with previous studies by

Sun et al. [8] and Phung et al. [7] that were the first to report the development of abnormal leaky blood vessels in the retina, skin, brain, limbs, and liver. They suggested that acute permeability in response to VEGF-A is not affected by myrAkt1. However, it leads to long term, low-level leakage with the formation of edema in adjacent tissue, such as the skin or muscle. While mean fBV was constantly higher in myrAkt1grafts, longitudinal measurements showed a gradual decrease in PS consistent with the observed blood vessel maturation.

Akt1 pro-angiogenic mechanisms observed in myrAkt1 grafts can include the following. 1) Reduced apoptosis, induced by the activation of survival signals in endothelial cells [6], can cause altered vascular remodeling and the formation of large blood vessels that cover most of the graft area. 2) Amplified endothelial cell proliferation can lead to blood vessel tortuosity and increased blood vessel density. 3) Increased permeability, a well-known VEGF-dependent, pro-angiogenic stimulus can occur. Leaky blood vessels are the hallmarks of activated endothelial cells in solid tumors [20]. It allows rapid extravasation of extracellular proteases that accompany blood vessels sprouting. Indeed, high mean PS levels were found in myrAkt1 grafts. 4) Activation of eNOS, a major endothelial-derived angiogenic mediator that controls vascular remodeling and tone by inhibiting the proliferation of vascular smooth muscle cells [21–23], promotes endothelial cells migration to newly formed blood vessels [24] and induces extracellular matrix degradation by metalloproteinases [25, 26].

Based on the results of the myrAkt1 transgenic model, we next aimed at pharmacological intervention to improve ovarian graft reperfusion. Simvastatin therapy has a pro-angiogenic effect through activation of the PI3K-Akt1-eNOS signaling pathway [9, 27]. By the administration of simvastatin, we successfully activated Akt1 and eNOS in the thigh muscle (ovarian graft transplantation site). Intraperitoneal injection of activated simvastatin, starting 1 day before grafting and continuing until 7 days thereafter, improved vascular density and accelerated blood vessel maturation, as is evident by reduced permeability. We found a significant effect of simvastatin treatment on the augmented improvement in fBV during the critical ischemic period from Day 2 to Day 7 after grafting. Although mean fBV on Day 2 was significantly higher in the controls, permeability of the vessels, mainly in the muscular rim of the graft, was higher in the simvastatin group. Increased permeability is expected in sites with active
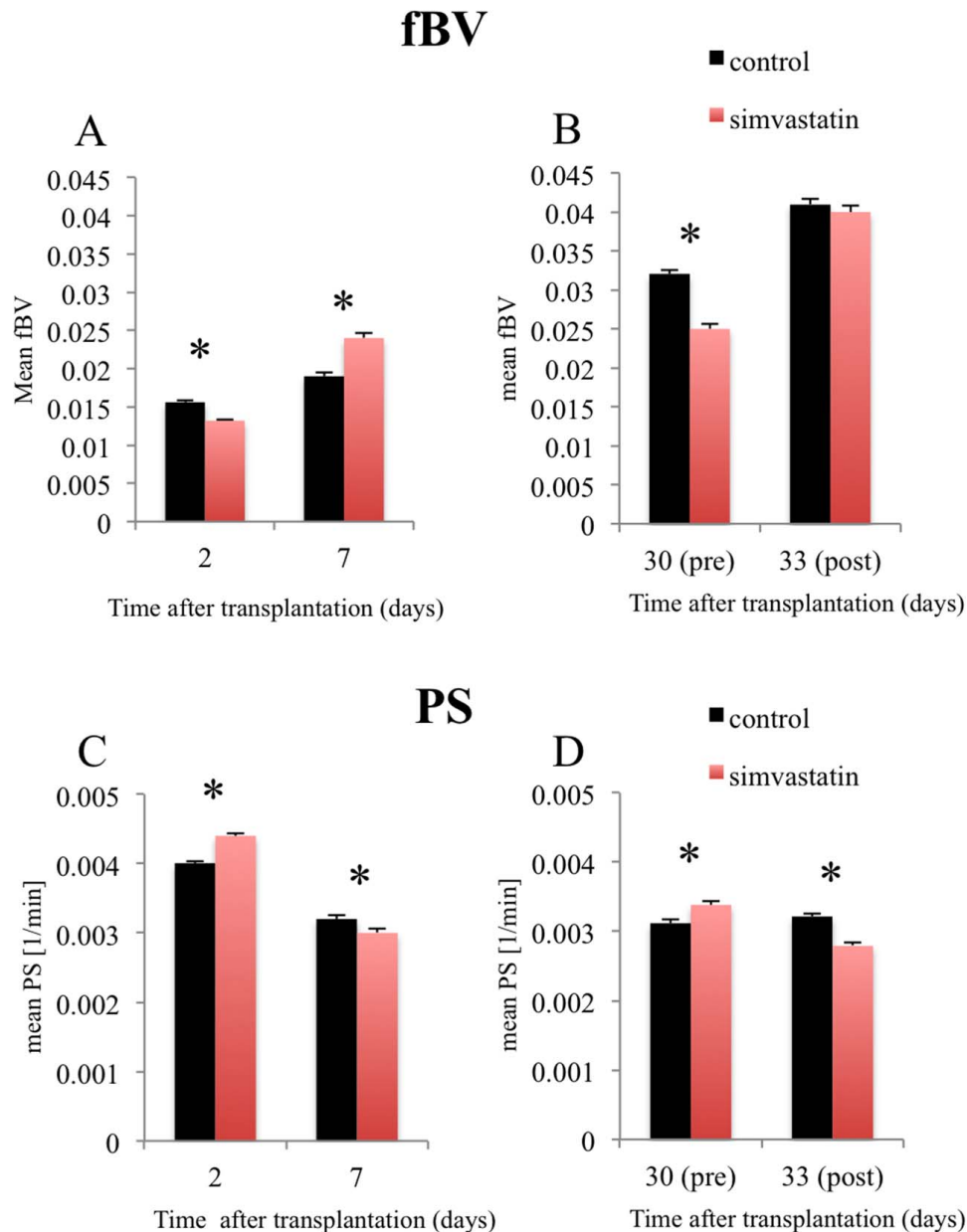
fBV

PS

FIG. 7. Augmented vascularization in response to simvastatin treatment. Recipient mice received daily IP injections of 0.1 mg/kg simvastatin or saline (control) starting 1 day before grafting and until 7 days thereafter. **A**) Simvastatin significantly improved mean blood volume fraction (fBV) from Day 2 after ovarian grafting to Day 7 and in response to superovulation between Days 30 and 33 (**B**). **C**, **D**) Decline in mean PS was found during these periods. Pre = presuperovulation with eCG/hCG; Post = 14–17 h after hCG administration (n = 7 each). *$P < 0.05$ by nested ANOVA. Data presented as mean ± SEM.

angiogenesis, whereas reduced permeability is found when mature functional vessels are formed [28]. Most importantly, at the time when revascularization of the graft was complete, 7 days after transplantation, grafts transplanted to animals treated with simvastatin had higher vascular density.

Next, we aimed at testing the ovarian reserve and the plasticity of the graft vasculature 30 days after transplantation, after the hormonal induction of superovulation. This dynamic testing for the ovarian graft reserve and angiogenic response can be used to estimate the success of ovarian grafting. Ovarian grafts transplanted in mice that received simvastatin significantly improved their fBV after superovulation compared to controls. Prior to eCG/hCG administration, mean fBV was lower in simvastatin-treated mice. Nevertheless, the hormonally induced angiogenic response of the graft was not impaired because we found significantly elevated vascular remodeling

and growth 14–17 h after hCG administration in animals treated with simvastatin. Blood vessel permeability in the simvastatin group showed similar trends at Days 2–7, with a decline in PS that can be attributed to accelerated blood vessel maturation. Normalized vascular density after superovulation, calculated from the signal of fluorescently tagged albumin (BSA-ROX) in patent blood vessels, was higher in the group treated with simvastatin. Therefore, simvastatin also resulted in superior vascular support after ovulation induction.

Ovarian grafts in animals treated with simvastatin showed a significantly reduction of follicle atresia. Superovulation yielded significantly higher numbers of corpora lutea per unit of graft volume and in recipients treated with simvastatin. The clinical implications of our findings include the possibility for improved graft reception and a higher ovulation rate following simvastatin administration to ovarian graft recipients, which
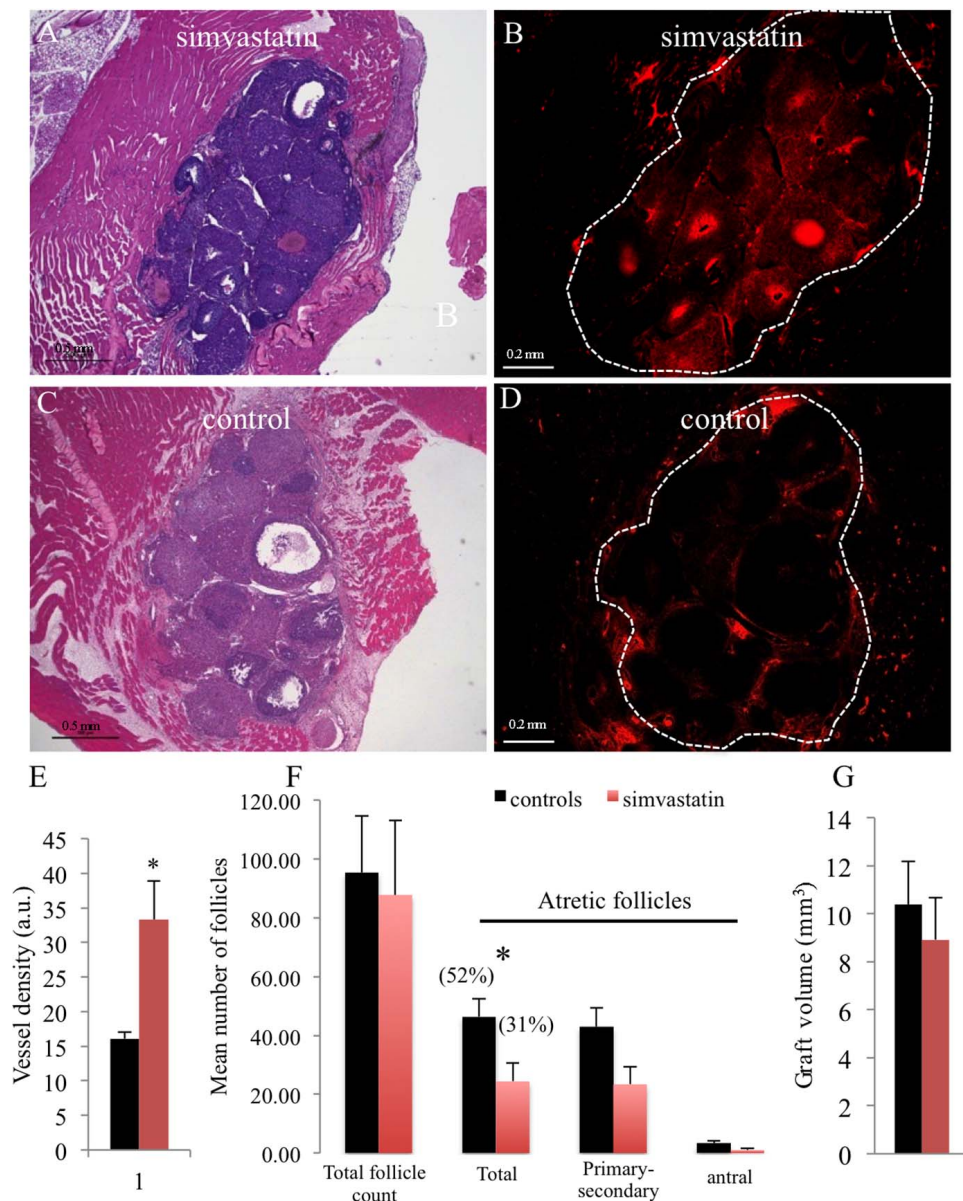
9

FIG. 8. Improved ovarian graft vascular and follicle density after simvastatin treatment. Grafts were treated with simvastatin from 1 day before grafting until 7 days thereafter. **A**, **C**) H&E stain. **B**, **D**) functional blood vessels depicted by fluorescence signal of BSA-ROX (red) injected 1 min prior to animal sacrifice. Dashed line outlines the graft area. Bar = 0.5 mm (**A**, **C**) and 0.2 mm (**B**, **D**). **E**) Mean normalized blood vessel density measured by fluorescence microscopy was about 2-fold higher in the simvastatin group compared to control. **F**) Mean total normal and atretic follicle counts in histological sections. Follicle atresia was significantly higher in the controls (percentage of atretic follicles from total follicle count). **G**) Mean ovarian graft volume, measured by MRI, was similar between the groups (n = 5–6 grafts in each group). *$P < 0.05$ by independent t-test. Data presented as mean ± SEM.

can increase the number of oocytes available for in vitro fertilization in patients undergoing fertility preservation treatment.

Primordial, antral, and total follicle densities were higher in animals treated with simvastatin, albeit it was not statistically significant. The same trend was found after correction for the nonvascular tissue of the graft. Limitations of our count that is based upon multilevel sampling in 120 μm increments could have masked differences in ovarian graft reserve that were the result of improved angiogenesis in the simvastatin group.

The results of this study clearly show that simvastatin administration to the recipient mouse can augment angiogenic response in ovarian grafts. At the same time, we hypothesize that other vascular protective mechanisms of eNOS can support the grafted tissue during the ischemic period, including:

antiplatelet aggregation activity that protects blood vessels from thrombosis [29], reduced vascular inflammatory response [30], and suppression of smooth muscle cells proliferation. Nitric oxide release from endothelial cells can suppress smooth muscle cells proliferation. Theoretically, the effect of simvastatin treatment could be attributed to its plasma cholesterol-lowering action or, alternatively, to another cholesterol-independent mechanism. Previous reports suggested that the pro-angiogenic effect of simvastatin is achieved at a low dosage without changing plasma cholesterol levels [31–34]. However, the low dosage of simvastatin that was used is not expected to change the plasma cholesterol levels, particularly when it was administered only for a short period of 8 days. Higher levels of phosphorylated eNOS were found after administration of 1 mg/kg. In our transplantation model, a

10

low dose of 0.1 mg/kg simvastatin was administered to ovarian graft recipients in order to minimize any potential cholesterol-lowering effect. Future studies with frozen-thawed ovarian grafts can be used to test the applicability of our findings for fertility preservation in cancer survivors and whether superior activation of eNOS, with higher doses of simvastatin, can further augment the graft angiogenic response.

This study represents the continuum from discovering the physiology of vascular remodeling in ovarian grafts to a transgenic model that reveals the main role of Akt1 in ovarian graft reception and ultimately to suggesting a new pharmaceutical therapy to improve fertility preservation among women survivors of cancer. Endothelial Akt1 activation promoted angiogenesis and the development of a unique population of new blood vessels that support the graft during the posttransplantation hypoxic period. Similarly, simvastatin therapy improves revascularization and vascular support of ovarian grafts. The pro-angiogenic effects reported here may extend beyond improving ovarian graft reception in fertility preservation and after further research could potentially be used for different organ or tissue transplantations.

ACKNOWLEDGMENT

REFERENCES

1. Donnez J, Dolmans MM, Pellicer A, Diaz-Garcia C, Sanchez Serrano M, Schmidt KT, Ernst E, Luyckx V, Andersen CY. Restoration of ovarian activity and pregnancy after transplantation of cryopreserved ovarian tissue: a review of 60 cases of reimplantation. Fertil Steril 2013; 99:1503–1513.
2. Israely T, Dafni H, Nevo N, Tsafriri A, Neeman M. Angiogenesis in ectopic ovarian xenotransplantation: multiparameter characterization of the neovasculature by dynamic contrast-enhanced MRI. Magn Reson Med 2004; 52:741–750.
3. Baird DT, Webb R, Campbell BK, Harkness LM, Gosden RG. Long-term ovarian function in sheep after ovariectomy and transplantation of autografts stored at −196 C. Endocrinology 1999; 140:462–471.
4. Somanath PR, Razorenova OV, Chen J, Byzova TV. Akt1 in endothelial cell and angiogenesis. Cell Cycle 2006; 5:512–518.
5. Cohen Y, Dafni H, Avni R, Raz T, Biton I, Hemmings B, Neeman M. In search of signaling pathways critical for ovarian graft reception: Akt1 is essential for long-term survival of ovarian grafts. Fertil Steril 2014; 101:536–544.
6. Shiojima I, Walsh K. Role of Akt signaling in vascular homeostasis and angiogenesis. Circ Res 2002; 90:1243–1250.
7. Phung TL, Ziv K, Dabydeen D, Eyiah-Mensah G, Riveros M, Perruzzi C, Sun J, Monahan-Earley RA, Shiojima I, Nagy JA, Lin MI, Walsh K, et al. Pathological angiogenesis is induced by sustained Akt signaling and inhibited by rapamycin. Cancer Cell 2006; 10:159–170.
8. Sun Y, Phung T, Shiojima I, Felske T, Upalakalin JN, Feng D, Kornaga T, Dor T, Dvorak AM, Walsh K, Benjamin LE. Microvascular patterning is controlled by fine-tuning the Akt signal. Proc Natl Acad Sci U S A 2005; 102:128–133.
9. Kureishi Y, Luo Z, Shiojima I, Bialik A, Fulton D, Lefer DJ, Sessa WC, Walsh K. The HMG-CoA reductase inhibitor simvastatin activates the protein kinase Akt and promotes angiogenesis in normocholesterolemic animals. Nat Med 2000; 6:1004–1010.
10. Israely T, Nevo N, Harmelin A, Neeman M, Tsafriri A. Reducing ischaemic damage in rodent ovarian xenografts transplanted into granulation tissue. Hum Reprod 2006; 21:1368–1379.
11. Luo C, Zuniga J, Edison E, Palla S, Dong W, Parker-Thornburg J. Superovulation strategies for 6 commonly used mouse strains. J Am Assoc Lab Anim Sci 2011; 50:471–478.
12. Sadeghi MM, Collinge M, Pardi R, Bender JR. Simvastatin modulates cytokine-mediated endothelial cell adhesion molecule induction: involvement of an inhibitory G protein. J Immunol 2000; 165:2712–2718.
13. Dafni H, Kim SJ, Bankson JA, Sankaranarayanapillai M, Ronen SM. Macromolecular dynamic contrast-enhanced (DCE)-MRI detects reduced vascular permeability in a prostate cancer bone metastasis model following anti-platelet-derived growth factor receptor (PDGFR) therapy, indicating a drop in vascular endothelial growth factor receptor (VEGFR) activation. Magn Reson Med 2008; 60:822–833.
14. Kalchenko V, Kuznetsov Y, Meglinski I, Harmelin A. Label free in vivo laser speckle imaging of blood and lymph vessels. J Biomed Opt 2012; 17:050502.
15. Bochner F, Fellus-Alyagor L, Kalchenko V, Shinar S, Neeman MA. Novel intravital imaging window for longitudinal microscopy of the mouse ovary. Sci Rep 2015; 5:12446.
16. Dafni H, Gilead A, Nevo N, Eilam R, Harmelin A, Neeman M. Modulation of the pharmacokinetics of macromolecular contrast material by avidin chase: MRI, optical, and inductively coupled plasma mass spectrometry tracking of triply labeled albumin. Magn Reson Med 2003; 50:904–914.
17. Van Eyck AS, Jordan BF, Gallez B, Heilier JF, Van Langendonckt A, Donnez J. Electron paramagnetic resonance as a tool to evaluate human ovarian tissue reoxygenation after xenografting. Fertil Steril 2009; 92:374–381.
18. Van Eyck AS, Bouzin C, Feron O, Romeu L, Van Langendonckt A, Donnez J, Dolmans MM. Both host and graft vessels contribute to revascularization of xenografted human ovarian tissue in a murine model. Fertil Steril 2010; 93:1676–1685.
19. Chen J, Somanath PR, Razorenova O, Chen WS, Hay N, Bornstein P, Byzova TV. Akt1 regulates pathological angiogenesis, vascular maturation and permeability in vivo. Nat Med 2005; 11:1188–1196.
20. Claesson-Welsh L, Welsh M. VEGFA and tumour angiogenesis. J Intern Med 2013; 273:114–127.
21. Garg UC, Hassid A. Nitric oxide-generating vasodilators and 8-bromo-cyclic guanosine monophosphate inhibit mitogenesis and proliferation of cultured rat vascular smooth muscle cells. J Clin Invest 1989; 83:1774–1777.
22. Cornwell TL, Arnold E, Boerth NJ, Lincoln TM. Inhibition of smooth muscle cell growth by nitric oxide and activation of cAMP-dependent protein kinase by cGMP. Am J Physiol 1994; 267:C1405–C1413.
23. Sarkar R, Meinberg EG, Stanley JC, Gordon D, Webb RC. Nitric oxide reversibly inhibits the migration of cultured vascular smooth muscle cells. Circ Res 1996; 78:225–230.
24. von der Leyen HE, Gibbons GH, Morishita R, Lewis NP, Zhang L, Nakajima M, Kaneda Y, Cooke JP, Dzau VJ. Gene therapy inhibiting neointimal vascular lesion: in vivo transfer of endothelial cell nitric oxide synthase gene. Proc Natl Acad Sci U S A 1995; 92:1137–1141.
25. Murrell GA, Jang D, Williams RJ. Nitric oxide activates metalloprotease enzymes in articular cartilage. Biochem Biophys Res Commun 1995; 206:15–21.
26. Trachtman H, Futterweit S, Garg P, Reddy K, Singhal PC. Nitric oxide stimulates the activity of a 72-kDa neutral matrix metalloproteinase in cultured rat mesangial cells. Biochem Biophys Res Commun 1996; 218:704–708.
27. Urbich C, Dernbach E, Zeiher AM, Dimmeler S. Double-edged role of statins in angiogenesis signaling. Circ Res 2002; 90:737–744.
28. Potente M, Gerhardt H, Carmeliet P. Basic and therapeutic aspects of angiogenesis. Cell 2011; 146:873–887.
29. Simon DI, Stamler JS, Jaraki O, Keaney JF, Osborne JA, Francis SA, Singel DJ, Loscalzo J. Antiplatelet properties of protein S-nitrosothiols derived from nitric oxide and endothelium-derived relaxing factor. Arterioscler Thromb 1993; 13:791–799.
30. Qian H, Neplioueva V, Shetty GA, Channon KM, George SE. Nitric oxide synthase gene therapy rapidly reduces adhesion molecule expression and inflammatory cell infiltration in carotid arteries of cholesterol-fed rabbits. Circulation 1999; 99:2979–2982.
31. Endres M, Laufs U, Huang Z, Nakamura T, Huang P, Moskowitz MA, Liao JK. Stroke protection by 3-hydroxy-3-methylglutaryl (HMG)-CoA reductase inhibitors mediated by endothelial nitric oxide synthase. Proc Natl Acad Sci U S A 1998; 95:8880–8885.
32. Sparrow CP, Burton CA, Hernandez M, Mundt S, Hassing H, Patel S, Rosa R, Hermanowski-Vosatka A, Wang PR, Zhang D, Peterson L, Detmers PA, et al. Simvastatin has anti-inflammatory and antiatherosclerotic activities independent of plasma cholesterol lowering. Arterioscler Thromb Vasc Biol 2001; 21:115–121.
33. Bea F, Blessing E, Bennett B, Levitz M, Wallace EP, Rosenfeld ME. Simvastatin promotes atherosclerotic plaque stability in apoE-deficient mice independently of lipid lowering. Arterioscler Thromb Vasc Biol 2002; 22:1832–1837.
34. Bea F, Blessing E, Shelley MI, Shultz JM, Rosenfeld ME. Simvastatin inhibits expression of tissue factor in advanced atherosclerotic lesions of apolipoprotein E deficient mice independently of lipid lowering: potential role of simvastatin-mediated inhibition of Egr-1 expression and activation. Atherosclerosis 2003; 167:187–194.